Switching Loss Reduction of PT- and NPT-IGBT

K. H. EDELMOSER & L. L. ERHARTT
Department of Power Electronics
Technical University Vienna
Gusshausstr. 27-29, A-1040 Wien
AUSTRIA

Abstract: - In order to keep the switching losses for high power applications (≥100A, ≥1000V) below acceptable levels, the switching actions have to proceed within microseconds. There with modern power switches very high switching speeds result (>1kA/µs, >5kV/µs), leading to considerable cost, e.g., for wireing and EMC measures. For hard switching operation, therefore, the switching losses limit the obtainable switching frequency and for switching frequencies above several kHz, overdimensioning, reduction of efficiency and excessive cost for heat removal result. Using the ZCS-ARCP, the quasi dual structure to the ZVS-ARCP [5], the turn-off losses in a test circuit have been eliminated almost completely [4]. The obtainable switching frequency is no longer determined by the switching losses but depends on the resonant frequency of the quenching circuit (which is chosen for good loss-reduction). The functioning of the ZCS-ARCP as well as the test circuit is described in [4,7,8] In the current paper the turn off behavior of the NPT-modules BSM100GB100D and BSM100GB170D as well as of the PT-module MG100Q2YS1 with equal ZCS-ARCP snubbers are investigated. A substantial part of the turn-off losses is given by the so-called tail-losses which depend on the lifetime of the minority carriers. The PT-type IGBTs are well suited for soft switching applications due to the high snubber effect of about 90%. *CSCC'99 Proceedings,* Pages:3851-3856

Key-Words: - PT-IGBT, NPT-IGBT, turn off switching behavior, ZCS-ARCP, switching loss reduction

1. Introduction

In order to keep the switching losses for high power applications (≥100A, ≥1000V) below acceptable levels, the switching actions have to proceed within microseconds. There with modern power switches very high switching speeds result (>1kA/µs, >5kV/µs), leading to considerable cost, e.g., for wireing and EMC measures. For hard switching operation, therefore, the switching losses limit the obtainable switching frequency and for the switching frequencies above several kHz, overdimensioning, reduction of efficiency and excessive cost for heat removal result.

Using the ZCS-ARCP the turn-off losses in a test circuit have been eliminated almost completely [4]. The obtainable switching frequency is no longer determined by the switching losses but depends on the duration of the tail current and the resonant frequency of the quenching circuit (which is chosen for good loss-reduction).

The ZCS-ARCP on the contrary to the ZVS-ARCP [5] is primarily a turn-off snubber. In the case of IGBTs a substantial part of the turn off losses is given by the so-called tail-losses which depend on the lifetime of the minority carriers.

In the current paper the turn off behavior of the NPT-modules BSM100GB100D and BSM100GB170D as well as of the PT-module MG100Q2YS1 with equal ZCS-ARCP snubbers are investigated.

2. Test Circuit and Measurement

Figure 1 shows the test circuit and the measured variables u_A (voltage across the lower switch $S_{A,N}$), switch current i_N and load current i_A. The main switching branch consists of an IGBT half-bridge S_A and an antiparallel diode D_A. There is no series impedance between the P and N branches, which are directly across the dc voltage source U_{ZK}. The load R_0,L_0 is connected to the center A of the main half bridge and to $U_{ZK}/2$.

The circuitry on the left side of the main module S_A is the ZCS-ARCP. Because only half bridge modules were available in the labaratory, the resonant tank L_R,C_R is switched on half the dc-link voltage $U_{ZK}/2$ via the autotransformer Tr and the auxiliary half

bridge S_H,D_H. This idea was first proposed in [6]. The resonant inductor L_R is realized with the stray inductance of the autotransformer. The functioning of the ZCS-ARCP as well as the test circuit is described in [4,7,8].

For the labaratory circuit in Fig.1. the following components and parameters have been selected:

U_{ZK} = 600V
R_0 = 90mΩ
D_{K1}, D_{K2} - BY255 (ITT)
D_{KP}, D_{KN} - BYT230PI-800 (SGS Thomson)
S_H, D_H - BSM50GB100D (Siemens)
S_A, D_A - MG100Q2YS1 (Toshiba)
Autotransformer - N = 10, two ferrite pairs of E65 cores
L_R = 3,6µH
C_R = 4*68nF (FKP1-capacitors, Wima)
f_S = 17kHz

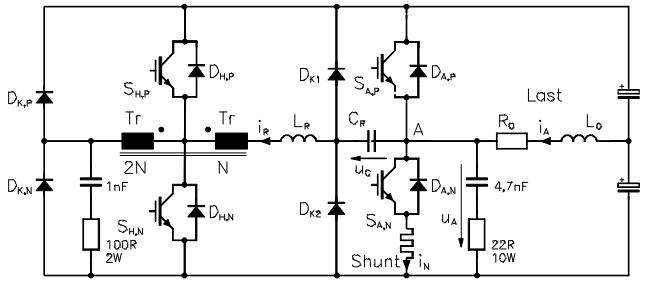

Fig.1. Laboratory circuit. The resonant tank L_R C_R is switched on halve the DC-link voltage $U_{ZK}/2$ via the autotransformer *Tr* and the auxiliary halve bridge module S_H, D_H.

The module S_A under test is mounted on a seperate heat sink being held at 110°C by a heater. The test circuit is operated in the burst mode (cf. Fig.2) such that the chip temperature lies only marginally above the heat sink temperature of 110°C.

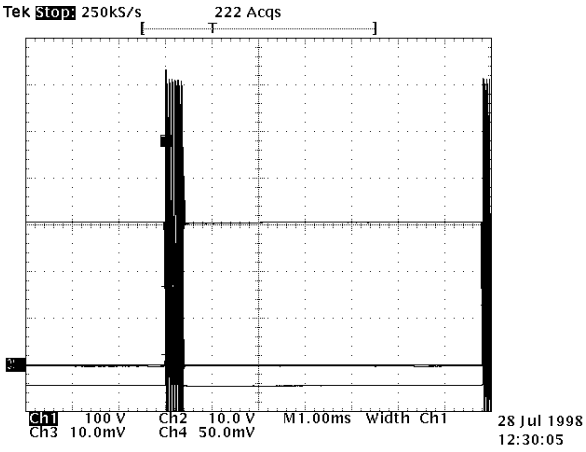

Figure 2: operation of the test circuit in burst mode

Initially, the 100A, 1000V module BSM100GB100D is used. Figure 3 shows the voltage u_A across the switch, the switch current i_N, load current i_A and gate voltage $u_{gH,N}$ of the auxiliary switch; by its turn-on the quenching of the main switch is initiated. The load current is measured with a balanced shunt. By checking the measurements of the load current i_A with a Tektronix 100A current probe the temperature offset of the copper shunt is eliminated for determining the switching losses.

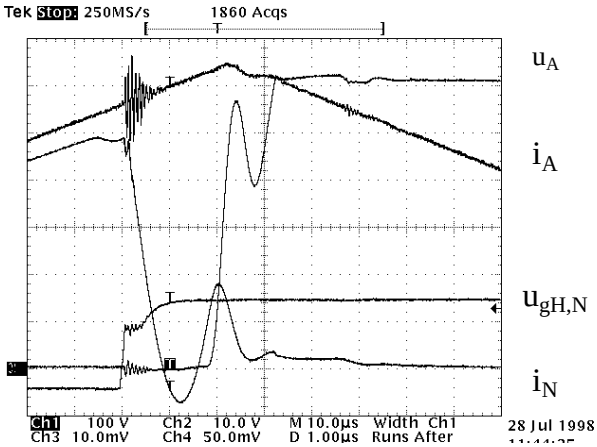

Figure 3: Commutation for partial load; the turn-off current I_{off} is per definition the amplitude of the load current i_A

As turn-off current I_{off} the amplitude of the load current i_A is used. The turn-off switching loss W_{off} resulting for each switching action consists of several contributions:

$$W_{off} = \sum_i W_{off,i} \tag{1}$$

The loss terms $W_{off,i}$ are determined for such a time interval Dt_i where the switch voltage u_A as well as the switch current i_N can be linearized with good approximation by

$$u_{S,i}(t) = U_{S0,i} + \frac{\Delta U_{S,i}}{\Delta t_i} \cdot t \tag{2}$$

and

$$i_{S,i}(t) = I_{S0,i} + \frac{\Delta I_{S,i}}{\Delta t_i} \cdot t \tag{3}$$

The loss integral for interval *i* with the duration Dt_i

$$W_{off,i} = \int_{\Delta t_i} u_{S,i}(t) \cdot i_{S,i}(t) \cdot dt \tag{4}$$

can then be calculated as

$$W_{off,i} = \left[\begin{array}{l} U_{S0,i} \cdot I_{S0,i} + \frac{1}{3} \cdot \Delta U_{S,i} \cdot \Delta I_{S,i} + \\ + \frac{1}{2} \cdot \left(U_{S0,i} \cdot \Delta I_{S,i} + I_{S0,i} \cdot \Delta U_{S,i} \right) \end{array} \right] \cdot \Delta t_i \tag{5}$$

The quantities $U_{S0,i}$, $I_{S0,i}$, $\Delta U_{S,i}$, $DI_{S,i}$ and Dt_i are shown in the respective figures and the corresponding tables.

The snubber effect E is defined as:

$$E = 1 - \frac{W_{off,soft}}{W_{off,hard}} \qquad (6)$$

Then the application of the snubber results in a reduction of the turn-off loss $P_{off,hart}=f_S*W_{off,hart}$ by $E* P_{off,hart}$.

3. The module BSM100GB100D

Figure 4 shows the commutation of the main switch down to the level of the tail current (about 12A). Channel two shows the gate signal of the main switch being turned off. An earlier turn off only would lead to higher losses and dos not reduce the tail current. The turn-off current amounts to about 84A (20A/Div.).

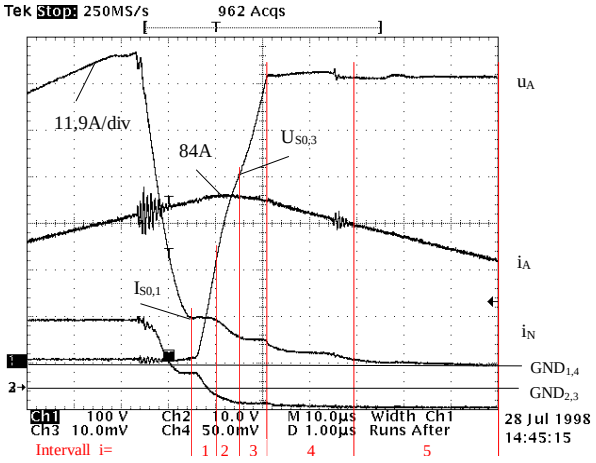

Figure 4: BSM 100 GB 100 D; resonant turn-off process, I_{off} = 84A, U_{ZK} = 610V, T_J = 110°C

Intervall	t_i	$U_{S0,i}$	$U_{S,i}$	$I_{S0,i}$	$I_{S,i}$	$W_{off,i}$
	[µs]	[V]	[V]	[A]	[A]	[mJ]
1	0,50	0	210	12,0	0	1,26
2	0,50	210	200	12,0	-5,9	1,35
3	0,50	410	200	6,1	0	0,62
4	1,90	610	0	3,0	0	3,48
5	3,00	610	0	0,9	-0,9	0,82

Table 1: Losses in Fig. 5, shown separately for each switching interval (resonant turn-off process)

$$W_{off,sn}(600V,80A) \approx \frac{600 \cdot 80}{610 \cdot 84} \cdot \sum_{i=1}^{5} W_{off,i} = 7mJ \qquad (7)$$

In comparison, Fig.5 shows the turn-off process for about 81A without snubber.

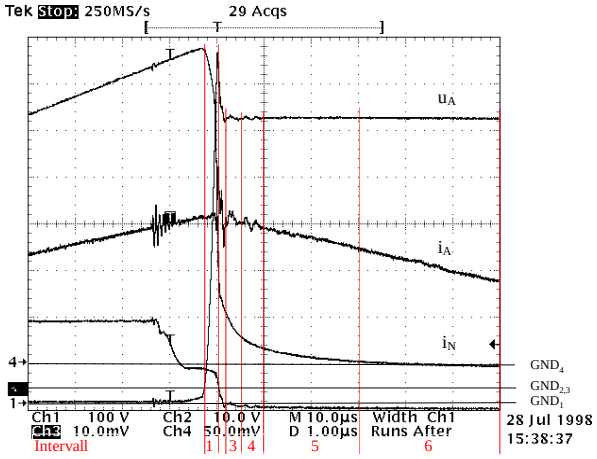

Figure 5: BSM 100 GB 100 D; hard turn-off I_{off} = 81A, U_{ZK} = 600V, T_J = 110°C

Intervall	t_i	$U_{S0,i}$	$U_{S,i}$	$I_{S0,i}$	$I_{S,i}$	$W_{off,i}$
	[µs]	[V]	[V]	[A]	[A]	[mJ]
1	0,25	0	760	81,0	-17	6,6
2	0,20	760	-160	19,0	-6,0	2,2
3	0,30	600	0	13,0	-6,5	1,8
4	0,50	600	0	6,5	-2,9	1,5
5	2,00	600	0	3,6	-3,1	2,5
6	3,00	600	0	0,5	-0,5	0,5

Table 2: Losses in Fig. 5, shown separately for each switching interval (hard turn-off process)

$$W_{off,tail}(600V,80A) \cong \frac{80}{81} \cdot \sum_{i=3}^{6} W_{off,i} \cong 6.1mJ \qquad (8)$$

$$W_{off,hard}(600V,80A) \cong \frac{80}{81} \cdot \sum_{i=1}^{6} W_{off,i} \cong 14.8mJ \qquad (9)$$

4. The Module BSM100GB170D

The measurement is also performed with 600V. For this purpose, already the triggering level for the desaturation control (short circuit protection!) had to be increased; for the bottom switch it had to be eliminated completely. This switch carries a current pulse for charging up the quenching capacitor (cf. Fig.6) at the first turn-on of the burst. The NPT-module goes into saturation more slowly than a PT-type. Figure 6 shows the turn-on process and the saturation of the power switch (forward voltage u_F in channel 2), occuring 3 microseconds later. The intelligent gate driver circuit [9] starts monitoring u_F 2µs after turn on.

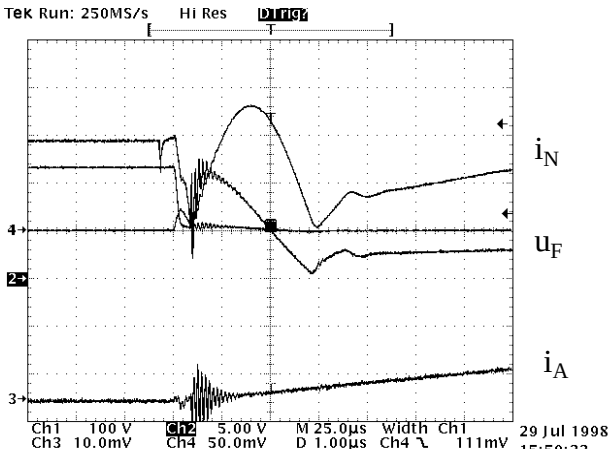

Figure 6: Turn-on behavior of the BSM100GB170D operating at 150V (c.f. channel 1).

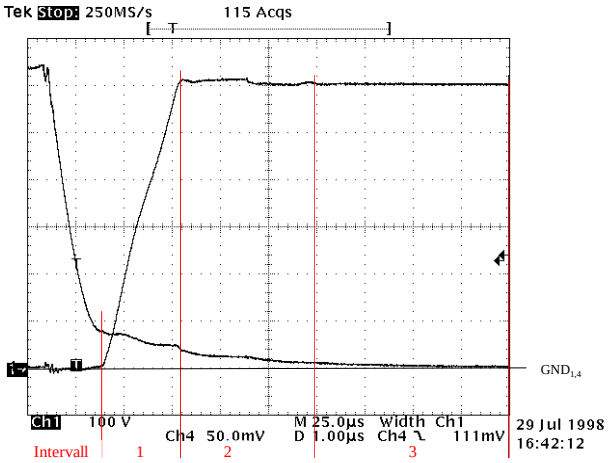

Figure 7: BSM100GB170D; resonant turn-off I_{off} = 80A, U_{ZK} = 600V, T_J = 110°C

Intervall	t_i	$U_{S0,i}$	$U_{S,i}$	$I_{S0,i}$	$I_{S,i}$	$W_{off,i}$
	[µs]	[V]	[V]	[A]	[A]	[mJ]
1	1,6	0	600	9,5	-4,4	3,2
2	2,8	600	0	4,2	-2,7	4,8
3	4,0	600	0	1,5	-1,5	1,8

Table 3: Losses in Fig. 7, shown separately for each switching interval (resonant turn-off process)

$$W_{off,sn}(600V,80A) \cong \sum_{i=1}^{3} W_{off,i} = 9.8mJ \qquad (10)$$

The quantities for calculating the resonant turn-off losses are shown in Figure 7. The hard turn-off process is shown in Fig. 8. For a more exact determination of the switching losses and for seperation into edge and tail losses for hard switching, the switching process shown in Fig. 9 has been decompressed in time once more. The time interval 1_T in Fig.9, starting after settling down of the switching overvoltage, is already attributed to the tail losses.

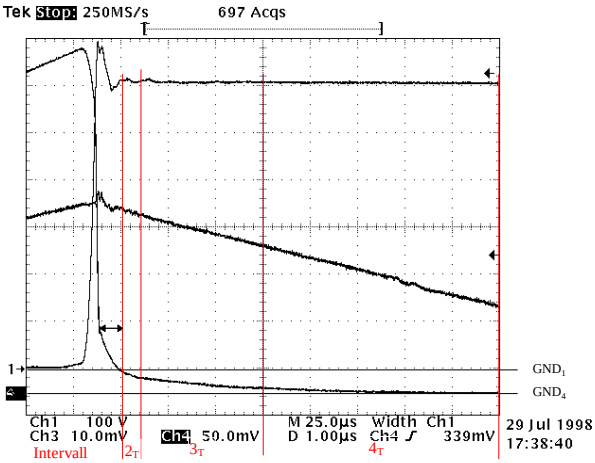

Figure 8: BSM100GB170D; hard turn-off I_{off} = 87A, U_{ZK} = 600V, T_J = 110°C; determination of the tail losses W_{offT} and of the entire switching losses $W_{off,hard}$ together with the losses W_{offS} during the switching edges from Fig.9

Intervall	t_i	$U_{S0,i}$	$U_{S,i}$	$I_{S0,i}$	$I_{S,i}$	$W_{off\ T,i}$
	[µs]	[V]	[V]	[A]	[A]	[mJ]
2_T	0,4	600	0	7,1	-2,9	1,4
3_T	2,6	600	0	4,2	-2,7	4,5
4_T	5,0	600	0	1,5	-1,5	2,3

Table 4: Losses in Fig. 8, shown separately for each switching interval (hard turn-off process)

$$W_{off,Tail}(600V,80A) \cong \frac{80}{87} \cdot \left(W_{offT,1} + \sum_{i=2}^{4} W_{offT,i} \right) = 8.6mJ$$

$$W_{off,hard}(600V,80A) \cong \frac{80}{87} \cdot \left(\sum_{i=1}^{6} W_{offS,i} + \sum_{i=1}^{4} W_{offT,i} \right) = 16mJ$$

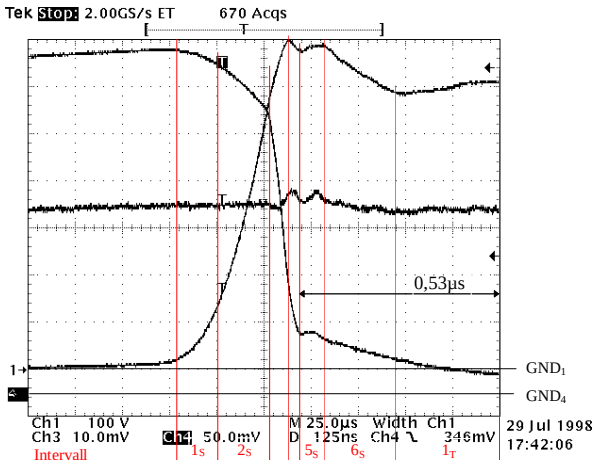

Figure 9: BSM100GB170D; hard turn-off I_{off} = 87A, U_{ZK} = 600V, T_J = 110°C; determination of the loss contributions W_{offS} during the switching edges

Intervall	t_i	$U_{S0,i}$	$U_{S,i}$	$I_{S0,i}$	$I_{S,i}$	$W_{offS,i}$
	[ns]	[V]	[V]	[A]	[A]	[mJ]
1_S	110	0	120	87,0	-4,2	0,56
2_S	145	120	450	82,8	-13,3	3,74
3_S	45	570	130	69,5	-40,9	1,38
4_S	30	700	-30	28,6	-12,9	0,46
5_S	60	670	20	15,7	0	0,64
6_S	190	690	-110	13,3	-4,7	1,33
7_S	275	580	20	8,6	-2,9	1,16

Table 5: Losses in Fig. 9, divided to each switching interval (hard turn-off process)

$$W_{off,s}(600V,80A) \cong \frac{80}{87}\cdot\left(\sum_{i=1}^{6} W_{offS,i}\right) = 7.5mJ \quad (13)$$

5. The Module MG100Q2YS9

The currents of the power switches of the PT-IGBT module MG100Q2YS9 are also commutated down to the level of the tail current.

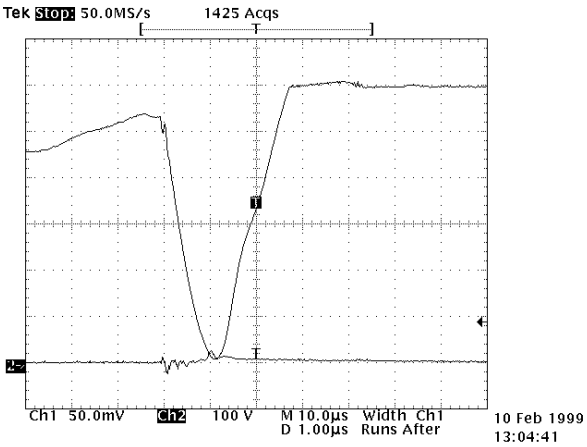

Figure 10: MG100Q2YS9; resonant turn-off, I_{off} = 74A, U_{ZK} = 600V, $T_J \cong$ 21°C

$$W_{off,snub} \cong 0mJ \quad (14)$$

To show the strong dependency of the tail current of PT-type IGBTs on the chip temperature, the cooler was not heated in Figure 10. Obviously, no tail current and no switching losses, respectively appears in this case.

High switching frequencies (around and above the upper audible frequency) can already be obtained without substantial increase of the switching losses. One can easily imagine that also this switching frequency limitation can be overcome in the future. Smallest intelligent snubbers for almost infinitely fast switches could reduce du/dt and di/dt to the presently manageable switching speeds; these could be easily handled then due to small construction dimensions.

Due to the heated cooler the chip temperature in Fig. 11 amounts about 100°C.

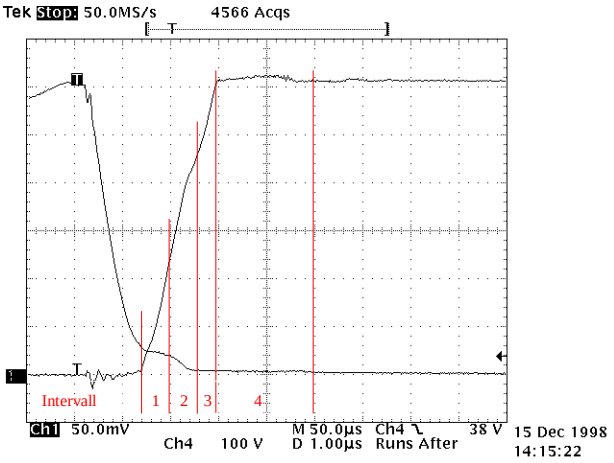

Figure 11: MG100Q2YS9; resonant turn-off, I_{off} = 84A, U_{ZK} = 610V, T_J = 100°C

Intervall	t_i	$U_{S0,i}$	$U_{S,i}$	$I_{S0,i}$	$I_{S,i}$	$W_{off,i}$
	[µs]	[V]	[V]	[A]	[A]	[mJ]
1	0,6	0	240	7,2	-2,4	0,4
2	0,6	240	220	4,8	-3,8	0,6
3	0,4	460	150	1	0	0,2
4	2,4	610	0	0,8	0	1,2

Table 6: Losses in Fig. 11, shown separately for each switching interval (hard turn-off process

$$W_{off,sn}(600V,80A) \approx \frac{600\cdot 80}{610\cdot 84}\cdot\sum_{i=1}^{5} W_{off,i} = 2{,}25mJ \quad (15)$$

6. Conclusion

The measurement results are compiled in table 7. The switching losses are approximately proportional to voltage and current. No noticeable error results due to the conversion form, e.g., 84A to 80A and 610V to 600V.

For a voltage stress being low as compared to the rated switch voltage the tail losses obviously are increased as compared to the losses during the switching edges. This makes also possible to explain the noticeable decreasing snubber effect with reduced voltage utilization. The tail losses for the BSM100GB170D result to 8.6mJ and, therefore, are almost equal to the losses resulting for resonant switching. In the Figures 4 and 7 it can be seen that the resonant turn-off of NPT-IGBT has almost no effect on its tail current.

With a reduction of the resonant frequency of the commutation circuit the obtainable switching frequency (presently about 50kHz) is reduced proportionally. This fact is not compensated by a substantial reduction of the switching losses (tail losses). Therefore, and due to a snubber effect of only 50%, the investigated NPT-IGBTs seem to be of marginal applicability for resonant operation.
In the case of the PT-IGBT the turn-off losses at 600V/80A amount to about 2.3mJ. Compared to the hard switching losses of the NPT-IGBT of about 14.8mJ the snubber effect E leads to 85%. Figure 10 represents the turn-off behavior at full load condition (74A) and room temperature (21°C) of the cooler. The load current is fully commutated, no tail current results. Due to almost negligible switching losses the snubber effect E reaches 100% in this case.

I_{off} = 80A, U_{ZK} = 600V T_j = 110°C	$W_{off,hart}$ [mJ]	W_{tail} [mJ]	$W_{off,entl}$ [mJ]	E [%]
BSM 100 GB 100 D	14,8	6,1	7,0	52
BSM 100 GB 170 D	16,0	8.6	9,8	39
MG100Q2YS1		2,25	2,25	85
MG100Q2YS1 (21°C)		≈0	≈0	99

Table 7: Losses of the modules

The ZCS-ARCP on the contrary to the ZVS-ARCP [5] is primarily a turn-off snubber. By splitting or by another arrangement of the commutation inductance also a turn-on snubber action is achieved [4,8]. (The voltage stress on the main switches rises then up to 1,5 times the DC-link voltage.) For the turn-off process at least the major part of the load current is guided away from the main switch; in partial load cases even a current in the opposite direction results (quenching). Especially for full load furthermore the rate of rise of the repetitive voltage is reduced, similar to the ZVS action. This explains the especially high snubber action which even rises with increasing load current.

References:

[1] W.McMurray, *Selection of Snubbers and Clamps to Optimize the Design of Transistor Switching Converters*, IEEE Transactions on Industry Applications, Vol. IA-16, No.4, 1980, pp.513-523.

[2] L.L. Erhartt, J.W. Kolar, G.W. Tuymer and F.C. Zach, *Comperative Study of the Switching Losses of an Isolated Gate Bipolar Transistor in PWM and Quasi Resonant Converter Applications*, PCIM, Nürnberg, 1991, pp. 195-207.

[3] K.E. Bornhard, *Switching Behavior of Pulse-Commutated GTO*, Power Electronics and Variable-Speed Drives Conference Record, 1988, pp. 83-86.

[4] L. Erhartt, *Neue Entlastungsschaltungen für Leistungshalbleiter in Halbbrückenanordnung und eine eigenintelligente Ansteuerstufe*, PhD thesis, TU Vienna, February 1998

[5] W. McMurray, *Resonant Snubbers with Auxiliary Switches*, IEEE Transactions on Industry Applications, Vol.32, No.2, March/April 1996, pp. 308-315.

[6] I. Barbi and D.C. Martins, *A True Pwm Zero-Voltage Switching Pole with Very Low Additional RMS Current Stress*, IEEE Power Electronics Specialists Conference, June 24-27, 1991, pp. 261-267.

[7] L.L. Erhartt, K. Edelmoser, M. Sedlacek and F.C. Zach, *A Novel Low-Loss Switching Method for Converters Using Turn-Off Power Switches*, 5th European Conference on Power Electronics and Applications, Brighton, UK, 13. bis 16. September 1993, Vol.3, S. 46-51

[8] K.H. Edelmoser, L.L. Erhartt, *Novel Low Loss Low Desturbance Zero Current Switching Pole*, Power Conversion and Intelligent Motion Conference, Nürnberg, 26.-28. Mai 1998, S. 209-217

[9] K.H. Edelmoser, L.L. Erhartt, F.C. Zach, *Floating, Flexible and Intelligent Gate Driver Circuit for IGBT Half-Bridge Modules up to 1200V, 100A*, Power Conversion and Intelligent Motion Conference, Nürnberg, 22.-24. June, 1992, S. 96-106